| | | |
|---|---|---|
| ESRF | **Experiment title:**<br>Full stress tensor determination in a textured 7150 aerospace alloy | **Experiment number**:<br>ME-515 |
| **Beamline**:<br>ID31 | **Date of experiment**:<br>from: 04/12/2002 to: 09/12/2002 | **Date of report**:<br>01/08/2003 |
| **Shifts: 6** | **Local contact(s)**:<br>Dr A. N. Fitch | *Received at ESRF:* |

**Names and affiliations of applicants** (* indicates experimentalists):

**V. Stelmukh*, L. Edwards* and S. Ganguly***

**Department of Materials Engineering, The Open University, Walton Hall, Milton Keynes MK7 6AA**

## Introduction:

Extensive research has been exploring a variety of advanced welding technologies (e.g. [1]) to reduce cost and provide innovative design options in airframe manufacturing. For damage tolerance of safety critical parts, it is vital that high quality joints of high strength precipitation hardened aluminium alloys currently considered for very large aircraft (VLA) wing construction exhibit as much resistance to crack growth as possible. In particular, the behaviour of fatigue cracks in terms of their location, growth rates and direction of propagation must be related to the residual stresses present in the welded structures. In order to obtain this knowledge accurate reliable methods enabling determination of the residual stress profiles around candidate welds must be developed. In our previous work [2, 3] a hybrid neutron/synchrotron diffraction technique was designed to optimize the mapping of the full 3D stress tensor in a Metal Inert Gas (MIG) welded 7150-W51(T6) aluminium alloy. The purpose of this experiment was to demonstrate that hard X-rays alone can be used for effective triaxial strain measurements in plates of this highly textured alloy, in the present case, welded using the variable polarity plasma arc (VPPA) process.

It has been traditionally believed that it is impractical to perform synchrotron through-thickness strain measurements on plate specimens in reflection (see e.g. [4]), as the X-ray path length is large ($=2D/\sin\theta$) for the usable diffraction angles ($\theta<12.5^{o}$) and depths, $D$, exceeding 1 mm. However, it is apparent that estimates of sufficient exposure times made for a texture-free material will not be valid for highly textured plates, where the most advantageous (hkl) reflection can be selected for the strain measurement in the normal (or through-thickness) direction (ND). 7XXX alloy plates are typically characterized by a strong texture in which *Brass*, {011} <211>, is usually one of the main components. This component strengthens with depth as shown by a number of investigators (see e.g. [5]) and can be inferred from the through-thickness intensity variation for the (220) peak (see Fig.1) taken from a previous neutron diffraction experiment [3]. Inverse pole figures obtained by the electron backscatter diffraction (EBSD) from the middle of the present AA7150 plate

are shown in Fig. 2, from which the presence of a much weaker *Cube*, {100} <001>, component can also be inferred.

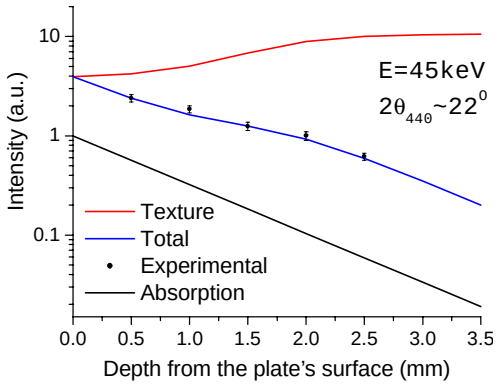


Fig 1: Through-thickness intensity variation of the (440) peak measured in reflection mode. Data represented by the red line were obtained from a previous neutron diffraction experiment.

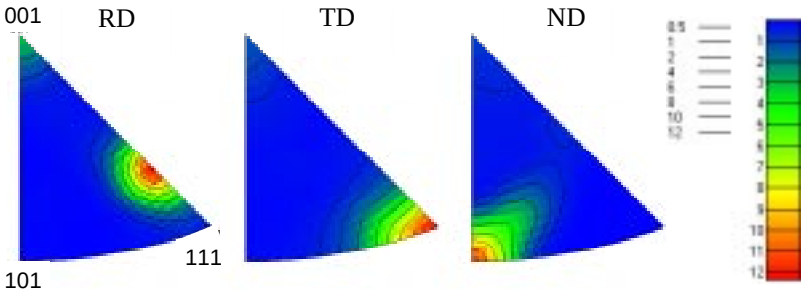


Fig 2: Inverse pole figures obtained for the middle of the parent plate using 10 - μm steps within a 1 mm square grid pattern. RD, TD and ND stand for the rolling, transverse and normal direction respectively.

## Specimen description and experimental details:

Two 12.6 mm thick 500 mm long AA7150 plates were VPPA welded in the W51 condition (solution treatment, quenching followed by stress relief by stretching (~2%) in the rolling direction) using the so-called "keyhole" mode [6], which provides for full-penetration single-pass welding. The weld orientation was parallel to the rolling direction (RD) of the parent plates. A conventional peak aging treatment was applied to the specimen following welding, equivalent to T6, that resulted in a T651 condition in the far field parent material and related conditions in the HAZ and fusion zone. Finally, a 280 mm square test-piece was cut off and then reduced in thickness to 7 mm by machining from both sides in increments of 0.5 mm to simulate a likely aerospace manufacturing process.

The experiment was conducted using 45keV X-rays. Outside the fusion zone, the measurements in reflection were found to be practically viable to the depths of 2.5 mm below the plate's surfaces (see Fig. 1), as individual count times per point did not exceed 30 sec. The (440) peak was used to measure the ND strain ($\varepsilon_{33}$), whereas the longitudinal ($\varepsilon_{11}$) and transverse ($\varepsilon_{22}$) strains were measured in transmission using the (422) and (222) peaks respectively. The "elastic stress free" reference measurements were made on a "comb" specimen, 120 mm long, removed by Electro Discharge Machining from another weld prepared under nominally identical conditions. The dimensions of each individual 'tooth' of the comb were 3.0×2.7 mm$^2$ in the LD-TD plane and 10.5 mm along ND. The allowance for a possible effect of the retained intergranular stresses on the macroscopic strain determination was made by measuring the reference specimen at orientations corresponding to equivalent measurements in the bulk material [7, 8].

## Results:

Figure 3a shows the lattice parameter distributions obtained by the deepest measurements in reflection. Data for the fusion zone (which approximately covers ±4 mm from the weld centre-line) are absent because the Brass texture component discontinues there. ND measurements from the through-thickness midline are possible but were not made, as they would require much longer counting times (see e. g. Fig. 1). Instead, the average of the shown distributions was used in the ND strain calculations since rather small through-thickness strain/stress gradients were found for all the measurement directions, as exemplified by the map of the longitudinal strain (see Fig. 3b). This map was generated by Gsharp 3.2 software using bilinear interpolation of several hundred individual strain values. Longitudinal tension is characterized by the presence of two distinct maxima in the HAZ (at about ±8 and ±18 mm from the weld centre-line) separated by a deep minimum in the fusion zone. Triaxial strain data obtained for the midline are shown in Fig. 4a. A noticeable scatter in the values of $\varepsilon_{22}$ in the fusion zone is attributable to the reduced number of grains in the gauge volume and related difficulties with texture average when using the (222) reflection characterized by a relatively small multiplicity factor ($P_{222}$=8, whereas $P_{422}$=24).

The measured strains, $\varepsilon_{ii} = (d_{hkl} - d_{hkl}^{ref})/d_{hkl}^{ref}$, were then converted to stresses using the reasonable assumption that the measurement directions were aligned with the principal stress axes, and Hooke's Law for isotropic solids:

$$\sigma_{ii} = \frac{E}{1+\nu}\varepsilon_{ii} + \frac{\nu E}{(1+\nu)(1-2\nu)}(\varepsilon_{11} + \varepsilon_{22} + \varepsilon_{33}) \qquad (1)$$

where the elastic modulus, $E$, was taken as 71 GPa and Poisson's ratio, $\nu$, as 0.35. The above formula and constants are found [8] to be suitable for the stress calculations when comparing their results with those obtained using a generalized Hooke's law for an aluminium plate with the (011) $[2\bar{1}1]$ ideal orientation (see e.g. [9]).

The calculated stress distributions are shown in Fig. 4b. The typical error in individual stress values, calculated using uncertainties of the peak positions for both the test-piece and the reference specimen, is about 2 MPa. The longitudinal stress profile largely inherits all the features of the corresponding strain distribution. At the weld centre-line the value of stress is estimated to be about 40 MPa. This can be done using the reasonable assumption that the behaviour of $\varepsilon_{33}$ in the fusion zone is similar to that of $\varepsilon_{22}$, that was subsequently confirmed in a neutron diffraction experiment (see Fig.3a). The maximum tensile longitudinal stresses, ranging from 140 to 150 MPa, are about 25% of the yield strength of AA7150-T651 alloy, which is 570 MPa at room temperature [10]. Starting from about ±22 mm, this stress declines rapidly with a distance from the weld centre-line, switching from tension to compression at 32-34 mm. This is near the outer boundaries of the HAZ (±37 mm), which were found by measuring hardness. The transverse stress is comparatively small and tensile at all locations. The latter is probably predetermined by the existing stress condition of the rolled plates [11] before welding.

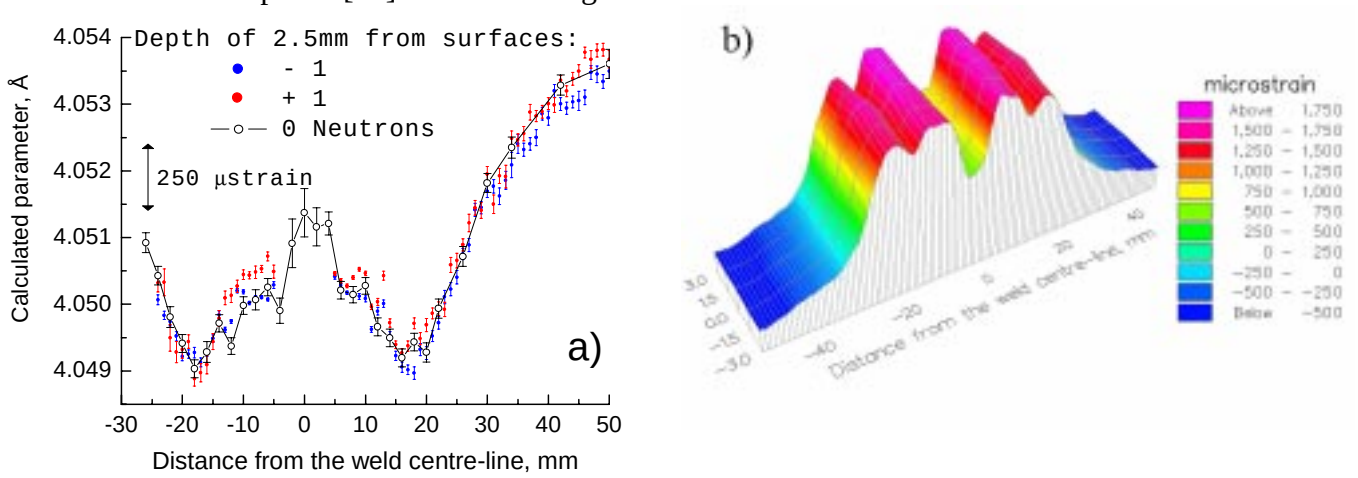


Fig 3: Lattice parameter variation obtained from the ND measurements (a). The corresponding neutron diffraction data (determined by the position of the (220) peak on time-of-flight spectra) were biased by + 0.0005Å (i.e. equivalent to about 100 μstrain). A 3D map of the longitudinal strain is given in (b).

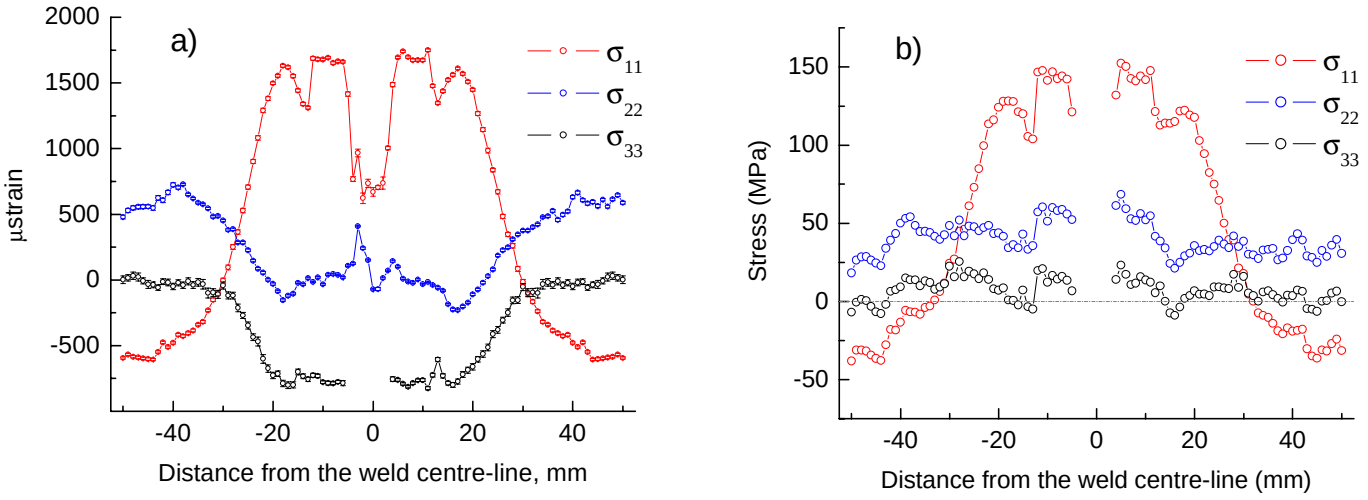


Fig 4: Midline strain (a) and stress (b) distributions.

The results of the $\sin^2\psi$ analysis for the reference comb suggest [8, 12] that macrostresses are still present in the reference specimen (see Fig. 5c). They are likely to be small in magnitude that was supported by the results of similar measurements made using laboratory X-rays (see Fig. 5d), where boundary condition, $\sigma_{11}=0$, holds. On the assumption that the uniaxial approximation for the stress condition ($\sigma_{11} = \sigma_{22} = 0$ and $\sigma_{33} \approx \pm 15$ MPa) in each "tooth" of the reference specimen is valid, the stress tensor found from the triaxial strain measurements can be corrected to eliminate the apparent disagreement between the $\sigma_{11}$-$\sigma_{33}$ distributions shown in Fig. 5 a and b. When applied, this correction results in a biaxial stress condition ($\sigma_{33}=0$) for the region in the HAZ corresponding to the first maximum of the longitudinal stress distribution. The highest tensile stress values, however, remain unchanged after this correction.

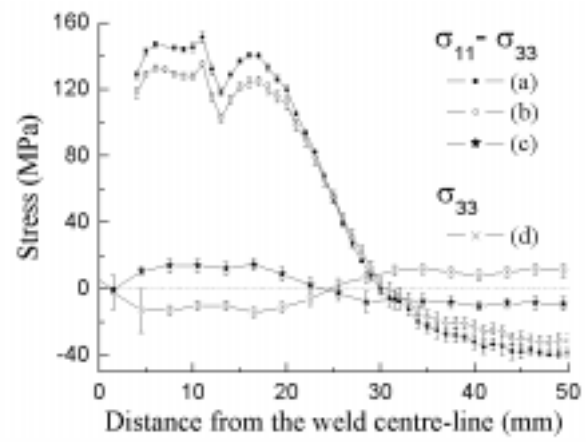


Fig. 5: Midline stress distributions for the weld (a, b) and reference comb (c, d) determined by the $\sin^2\psi$ method (a, c, d) and from triaxial stress measurements (b).

## References:


[1] Mendez, P.F. and Eagar, T.W. (2001) "Welding processes for aeronautics". *Advanced Materials & Processes*, 5, pp. 39-43

[2] Edwards, L; Stelmukh, V; Santisteban, J.R. and Ganguly, S. *Design and Durability of welded aircraft. ESRF report of Experiment ME-281: http://ftp.esrf.fr/pub/UserReports/21151_B.pdf*

[3] Stelmukh, V.; Edwards, L; Santisteban, J.R.; Ganguly, S. and Fitzpatrick, M.E. (2002) "Weld Stress Mapping Using Neutron and Synchrotron X-ray Diffraction", *Materials Science Forum*, 404-407, pp. 599-604

[4] Webster, P.J.; Oosterkamp, L.D.; Browne, P.A.; Hughes, D.J.; Kang W.P.; Withers, P.J. *et al.* (2001) "Synchrotron X-ray residual strain scanning of a friction stir weld", *J. Strain Anal. Eng.*, 36, pp. 61-70

[5] Stelmukh, V. and Edwards, L. (2002) "Optimizing Neutron Strain Scanning by the Use of Electron Backscatter Diffraction", *Microscopy&Analysis* , 91, pp. 15-16

[6] Cary, H. B. (1998). *Modern Welding Technology*, 4th edn, Prentice-Hall

[7] Krawitz, A.D. and Winholtz, R.A. (1994) "Use of position-dependent stress-free standard for diffraction stress measurements", *Mater. Sci. Eng. A*, 185, pp. 123-130

[8] Stelmukh, V.A. (2003) "Neutron and Synchrotron X-ray Residual Stress Mapping of 7XXX Aluminium Alloy Aerospace Welds ", Ph.D. Thesis (submitted), The Open University

[9] Hauk, V. (1997). *Structural and residual stress analysis by nondestructive methods.* Elsevier, Amsterdam

[10] Lin, J.; Stelmukh, V.; Ganguly, S.; Edwards, L.; Irving, P.E. (2003) "The effects of residual stress and HAZ on fatigue crack growth in MIG welded 2024 and 7150 Aluminium" To be published in *Fatigue and Fracture of Engineering Materials and Structures*

[11] Prime, M.B. and Hill, M.R. (2002) "Residual stress, stress relief, and inhomogeneity in aluminium plate", *Scripta Mater.*, 46, pp. 77-82

[12] Stelmukh, V.; Edwards, L. and Ganguly, S. (2003) "Full Stress Tensor Determination in a Textured Aerospace Aluminium Alloy Plate Using Synchrotron X-ray Diffraction", submitted for publication in a special edition of *Textures and Microstructures*